INTERNATIONAL JOURNAL OF ADVANCED STUDIES
IN COMPUTER SCIENCE AND ENGINEERING
IJASCSE VOLUME 6 ISSUE 2, 2017
02/28/2017

Modeling, Riccati-Sylvester Decoupling and Digital Multiloop Control of 3-DoF Gimbaled Stabilizing Platform (Part-I)

Faisal Mehmood, Tehreem Zahra, Zehera Batool, Arslan Arshad
Department of Electrical Engineering
COMSATS Institute of Information Technology
Wah 47040, Pakistan

***Abstract*—This article presents the design and control of a 3 Degrees of Freedom (DoF) gimbaled stabilizing platform. The nonlinear system dynamics are modelled in the detail. The nonlinear quadruple of the system is simulated in MATLAB and is linearized using the Jacobian technique. The system order reduction is performed using Riccati-Sylvester transform. The decoupled system is simulated and a novel adaptive control algorithm is designed to regulate the position of the platform in 3-DoF. The experimental validation of the theoretically proposed controller is also presented by implementing the discrete time realization of the control algorithm using a digital controller interfaced in the real-time, using MATLAB/Simulink, in the Rapid Control Prototyping (RCP) mode of operation. The feasibility of the proposed design is theoretically and experimentally verified by its efficiency comparison with the classical techniques and satisfactorily stable closed loop responses.**

Keywords-Riccati-Sylvester transformation; 3-DoF-gimbal; stabilizing plateform; Rapid Control Prototyping; adaptive control

I. INTRODUCTION

An inertial stabilized platform is one of the most important parts of modern tracking system. The areas of applications include but are not limited to defense, aerial photography, satellite imaging, industrial measurements etc. In platform stabilization system, the platform, where any desired object can be placed, is to be maintained at a fixed reference level although there is change in system dynamics and position [1]. A 3-Axis Gimbal structure is used to inertially stabilize a platform which can also be used to track a fixed or moving point in space with the help of other sensors [2].

A lot of research work has been done owing to the importance of this system in the field and its challenging dynamic behavior to be controlled. However, the detailed modeling of this system, including the intricate geometric relations for the moment of inertia of gimbals, has not emphasized much in the literature. Secondly, the dynamics of the system are not only nonlinear but also coupled. Riccati-Sylvester differential equations have already been a topic of interest for the disturbance decoupling and optimal decentralized control problems [3]. They have also been successfully employed in the problems involving observer design [4,5], suboptimal tracking control [6] and nonlinear systems with mismatched uncertainties [7]. The real domain of application of Riccati-Sylvester differential equations is the Riccati-Sylvester transform that can be used to partially, fully or selectively decoupled a given dynamic system [8]. This work considers a procedure of Riccati-Sylvester transformation for selective decoupling of the system dynamics.

Various control techniques have been implemented in the literature to stabilize a 3-DoF gimbal. Fuzzy logic has been implemented in [9]. Embedded sensor fusion and moving-average filter based methodologies are employed in [10]. Self-Adaptive Fuzzy Control is used in [11]. Takagi-Sugeno fuzzy PD controller are used in [12]. We have presented a simpler procedure involving ARM-Cortex-M embedded processor and Matlab, to develop a Rapid Control Prototyping (RCP) platform to design and test a Multiloop digital control strategy. The resulting control algorithm is not only flexible, with respect to the available degrees of freedom in terms of tunable controller parameters, but also very reliable under external disturbances.

In the part I of this research, a detailed nonlinear model of 3-DoF stabilizing platform will be developed, followed by linearization and simulation.

II. EXPERIMENTAL SETUP

A 3-DoF stabilizing gimbal platform is shown in Fig. 1. This physical setup consists of four parts

1. The fixed frame (as a semi annular ring) is solidly coupled to the body frame, that in turn is fixed to some carrier e.g. missile, aircraft, sea-ship or ground vehicle etc.
2. The outer gimbal (as full annular ring) is connected to the fixed frame through bearing at the points

P_1 and P_2, and it is solidly coupled to the shaft of gear DC motor M_1 at point P_2. The stator of the motor is connected with screws to the fixed frame.

3. The inner gimbal (as full annular ring) connected to the outer gimbal through bearing at the points P_3 and P_4, and it is solidly coupled to the shaft of the gear DC motor M_2 at the point P_3. The stator of the motor is connected with screws to the outer gimbal.
4. The stabilized platform (as a thin plate) is connected to the inner gimbal through the bearing at points P_5 and P_6, and it is solidly coupled to the shaft of gear DC motor M_3 at the point P_5. The stator of the motor is connected with screws to the inner gimbal.

A sensor assembly housing on the stabilized platform carries an Inertial Measurement Unit (IMU). Its contains three axis accelerometer, three axis gyroscope and three axis magnetometer with their signals fused using the extended Kalman filter to generate the Euler angles and the Euler rated, hence determining the attitude of the stabilized platform (e.g. roll, pitch and Yaw).

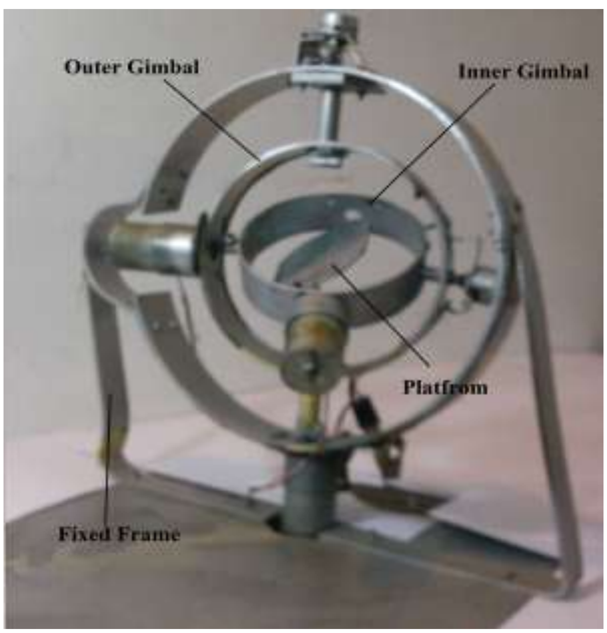

Figure 1. 3-DoF gimbal platform hardware setup.

III. System Dynamics

A. Frames of reference

To describe the system dynamics, four frames of reference are required, given by:

1. Body frame β, defined by (X_B, Y_B, Z_B) axis.
2. Outer Gimbal Frame ξ_ψ, defined by (X_ψ, Y_ψ, Z_ψ) axis.
3. Inner Gimbal Frame ξ_ϕ defined by (X_ϕ, Y_ϕ, Z_ϕ) axis.
4. Stabilized Platform Frame ξ_θ, defined by (X_θ, Y_θ, Z_θ) axis.

These frames of reference are related by standard rotational matrixes.

B. Moment of inertia

1) Stabilized platform moment of inertia

The stabilized plate form in Fig. 1 can be considered as a thin plate as shown in Fig. 2.

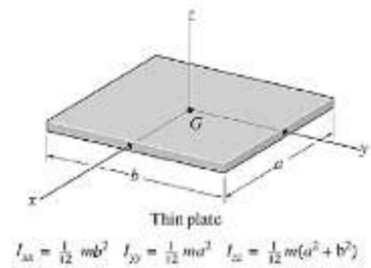

Figure 2. The moment of inertia of a thin plate.

The principle moments of inertia of the platform in ξ_θ are given by,

$$\begin{aligned} I_{PX_\theta} &= M_P a^2/12 \\ I_{PY_\theta} &= M_P b^2/12 \\ I_{PZ_\theta} &= M_P (a^2+b^2)/12 \end{aligned} \tag{1}$$

Translating these moments of inertia in β we get,

$$\begin{aligned} I_{PX_B} &= M_P a^2/12 \\ I_{PY_B} &= M_P (a^2\sin^2\theta + b^2)/12 \\ I_{PZ_B} &= M_P (a^2(\sin^2\phi\sin^2\theta + \cos^2\theta) + b^2\cos^2\phi)/12 \end{aligned} \tag{2}$$

Since the Euler angles $[\theta\ \phi\ \psi]^T$ and the Euler rates $[\dot\theta\ \dot\phi\ \dot\psi]^T$ are defines in β, so we rename moment of inertia along body axis as,

$$I_{PX_B} = I_{P\theta},\ I_{PY_B} = I_{P\phi},\ I_{PZ_B} = I_{P\psi} \tag{3}$$

2) Inner gimbal moment of inertia

The inner gimbal can be considered as an annular ring similar to one shown in Fig. 3.

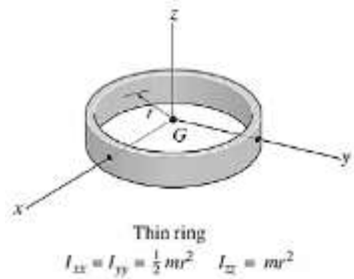

Figure 3. The moment of inertia of an annular ring.

The moment of inertia in ξ_ϕ and β are given by,

$$I_{IGX_\phi} = I_{IGY_\phi} = M_{IG} R_i^2 / 2 = I_{IGY_B} = I_{IG\phi}$$
$$I_{IGZ_\phi} = M_{IG} R_i^2 \qquad (4)$$
$$I_{IGZ_B} = M_{IG} (\sin^2 \phi + 1) / 2 = I_{IG\psi}$$

3) Outer gimbal moment of inertia

The outer gimbal can also be considered as an annular ring similar to one shown above in Fig. 3. The moment of inertia in ξ_ψ and β are given by,

$$I_{OGZ_\psi} = I_{OGY_\psi} = M_{IG} R_i^2 / 2 = I_{OGZ_B} = I_{OG\psi} \qquad (5)$$
$$I_{OGX_\psi} = M_{OG} R_i^2$$

4) DC motor dynamics

The electrical part of a PMDC motor, which is selected actuator, can be modeled as a series RL-back-EMF circuit along with the mechanical coupling as shown in Fig. 4

The same model is used for three motors so in the following modeling equation we have in general $\alpha = \theta, \phi, \psi$ and κ_m is back EMF constant and $\kappa_{\tau\alpha}$ is torque constant.

$$L_m \frac{d\tau_\alpha}{dt} + R_m \tau_\alpha = -\kappa_m \kappa_{\tau\alpha} \frac{d\alpha}{dt} + \kappa_{\tau\alpha} E_\alpha \qquad (6)$$

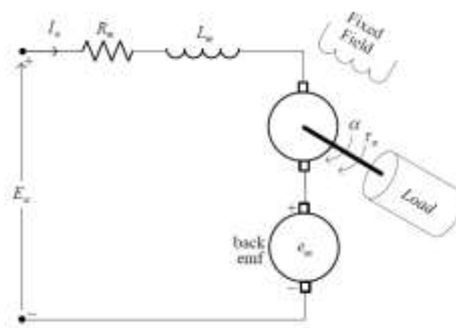

Figure 4. PMDC motor model.

Rewriting above equation separately for three motors we get,

$$L_{m1} \frac{d\tau_\theta}{dt} + R_{m1} \tau_\theta = -\kappa_{m1} \kappa_{\tau\theta} \frac{d\theta}{dt} + \kappa_{\tau\theta} E_\theta$$
$$L_{m2} \frac{d\tau_\phi}{dt} + R_{m2} \tau_\phi = -\kappa_{m2} \kappa_{\tau\phi} \frac{df}{dt} + \kappa_{\tau\phi} E_\phi \qquad (7)$$
$$L_{m3} \frac{d\tau_\psi}{dt} + R_{m3} \tau_\psi = -\kappa_{m3} \kappa_{\tau\psi} \frac{d\psi}{dt} + \kappa_{\tau\psi} E_\psi$$

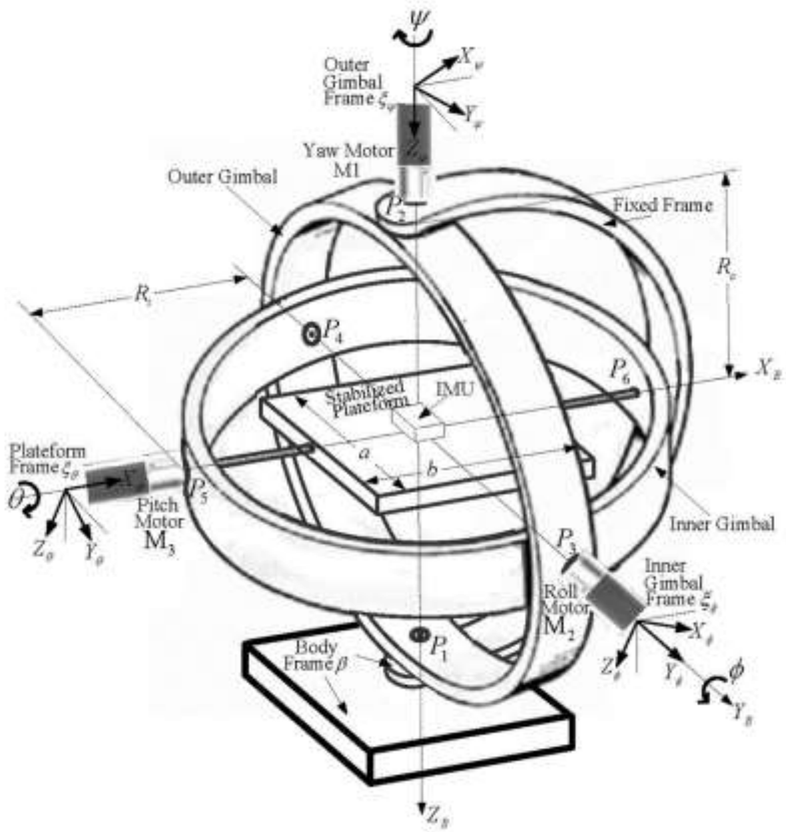

Figure 5. 3-DoF gimbal platform illustrative physical setup.

5) Gimbaled platform Model

The gimbaled platform dynamic equations, in the body frame β, are given by familiar Euler's equations as,

$$\frac{d^2\theta}{dt^2} = -\frac{d\phi}{dt}\frac{d\psi}{dt} + \frac{1}{I_{P\theta}}\left(-B_\theta\frac{d\theta}{dt} + \tau_\theta\right)$$
$$\frac{d^2\phi}{dt^2} = -\frac{d\theta}{dt}\frac{d\psi}{dt} + \frac{1}{I_{P\phi} + I_{IG\phi}}\left(-B_\phi\frac{d\phi}{dt} + \tau_\phi\right) \quad (8)$$
$$\frac{d^2\psi}{dt^2} = -\frac{d\theta}{dt}\frac{d\phi}{dt} + \frac{1}{I_{P\psi} + I_{IG\psi} + I_{OG\psi}}\left(-B_\psi\frac{d\psi}{dt} + \tau_\psi\right)$$

Where with $\alpha = \theta, \phi, \psi$ and,

B_α = frictional constant

τ_α =torque supplied by PMDC motors.

$\frac{d\theta}{dt}\frac{d\psi}{dt}$ =gyroscopic moment term during pitch

$\frac{d\theta}{dt}\frac{d\psi}{dt}$ = gyroscopic moment term during roll

$\frac{d\theta}{dt}\frac{d\phi}{dt}$ = gyroscopic moment term during yaw

$I_\theta = I_{P\theta}$ =Net moment of inertia for the pitch PMDC motor

$I_\phi = I_{P\phi} + I_{IG\phi}$ = Net moment of inertia for the roll PMDC motor

$I_\psi = I_{P\psi} + I_{IG\psi} + I_{OG\psi}$ = Net moment of inertia for the yaw PMDC motor

Rearranging the terms in the system dynamics (7) and (8), we get the complete non-linear system dynamic model as given,

$$\frac{d^2\theta}{dt^2} = -\frac{B_\theta}{I_\theta}\frac{d\theta}{dt} - \frac{d\phi}{dt}\frac{d\psi}{dt} + \frac{1}{I_\theta}\tau_\theta$$
$$\frac{d^2\phi}{dt^2} = -\frac{B_f}{I_f}\frac{d\phi}{dt} - \frac{d\theta}{dt}\frac{d\psi}{dt} + \frac{1}{I_f}\tau_\phi$$
$$\frac{d^2\psi}{dt^2} = -\frac{B_\psi}{I_\psi}\frac{d\psi}{dt} - \frac{d\theta}{dt}\frac{d\phi}{dt} + \frac{1}{I_\psi}\tau_\psi \qquad (9)$$
$$\frac{d\tau_\theta}{dt} = -\frac{R_{m1}}{L_{m1}}\tau_\theta - \frac{\kappa_{m1}\kappa_{\tau\theta}}{L_{m1}}\frac{d\theta}{dt} + \frac{\kappa_{\tau\theta}}{L_{m1}}E_\theta$$
$$\frac{d\tau_\phi}{dt} = -\frac{R_{m2}}{L_{m2}}\tau_\phi - \frac{\kappa_{m2}\kappa_{\tau\phi}}{L_{m2}}\frac{d\phi}{dt} + \frac{\kappa_{\tau\phi}}{L_{m2}}E_\phi$$
$$\frac{d\tau_\psi}{dt} = -\frac{R_{m3}}{L_{m3}}\tau_\psi - \frac{\kappa_{m3}\kappa_{\tau\psi}}{L_{m3}}\frac{d\psi}{dt} + \frac{\kappa_{\tau\psi}}{L_{m3}}E_\psi$$

6) State-space nonlinear dynamics:

We make the following state variable assignment to system (9),

$$x_1 = \theta,\quad x_2 = \dot{\theta},\quad x_3 = \phi,\quad x_4 = \dot{\phi},\quad x_5 = \psi$$
$$x_6 = \dot{\psi},\quad x_7 = \tau_\theta,\quad x_8 = \tau_\phi \quad x_9 = \tau_\psi \qquad (10)$$

The input variables assignment is given by,

$$u_1 = E_\theta,\ u_2 = E_\phi,\ u_3 = E_\psi \qquad (11)$$

The output variables assignment is given by,

$$y_1 = x_1,\ y_2 = x_2,\ y_3 = x_3,$$
$$y_4 = x_4,\ y_5 = x_5,\ y_6 = x_6 \qquad (12)$$

Using (10) through (12) in (9), we get,

$$\dot{x}_1 = x_2$$
$$\dot{x}_2 = -\frac{B_\theta}{I_\theta}x_2 - x_4x_6 + \frac{1}{I_\theta}x_7$$
$$\dot{x}_3 = x_4$$
$$\dot{x}_4 = -\frac{B_\phi}{I_\phi}x_4 - x_2x_6 + \frac{1}{I_\phi}x_8$$
$$\dot{x}_5 = x$$
$$\dot{x}_6 = -\frac{B_\psi}{I_\psi}x_6 - x_2x_4 + \frac{1}{I_\psi}x_9$$
$$\dot{x}_7 = -\frac{R_{m1}}{L_{m1}}x_7 - \frac{\kappa_{m1}\kappa_{\tau\theta}}{L_{m1}}x_2 + \frac{\kappa_{\tau\theta}}{L_{m1}}u_1$$
$$\dot{x}_8 = -\frac{R_{m2}}{L_{m2}}x_8 - \frac{\kappa_{m2}\kappa_{\tau\phi}}{L_{m2}}x_4 + \frac{\kappa_{\tau\phi}}{L_{m2}}u_2$$
$$\dot{x}_9 = -\frac{R_{m3}}{L_{m3}}x_9 - \frac{\kappa_{m3}\kappa_{\tau\psi}}{L_{m3}}x_6 + \frac{\kappa_{\tau\psi}}{L_{m3}}u_3 \qquad (13)$$

The non-linear system (13) can be represented by standard nonlinear system notation as,

$$\dot{\underline{x}} = \underline{F}(\underline{x},\underline{u}) \qquad (14)$$

Output dynamics are linear in (12) and can be represented by,

$$\underline{y} = C\underline{x} + D\underline{u} \qquad (15)$$

The values of various system constants in (13) and the gimbaled platform dimensions to be used in moment of inertia calculations are given in Table I. Here the subscript i, with the values 1. 2 and 3, represents parameters of the three PMDC motors that are identical and the angle α can be θ, ϕ or ψ.

TABLE I. VALUES OF SYSTEM PARAMETERS

Parameter	Value
M_p	$0.25Kg$
a	$0.15m$
b	$0.2m$
R_i	$0.25m$
R_o	$0.27m$
B_θ	0.002 Nm/ rad/ sec
B_ϕ	0.004 Nm/ rad/ sec
B_ψ	0.006 Nm/ rad/ sec
R_{mi}	4 Ohm
L_{mi}	0.007 H

Parameter	Value
κ_{mi}	0.5V/rad/sec
$\kappa_{\tau a}$	0.5Nm/A
M_{IG}	0.5Kg
M_{OG}	0.5Kg

C. *Nonlinear Simulation*

The system in (12) and (13) is implemented in Simulink in Fig. 6. The simulation results for step inputs to three motors, applied successively with delay, are shown in Fig. 7 and Fig. 8. It is clearly evident that system has coupled dynamics as one input effects all other outputs. The Euler rates are stable due to back-EMF in motors, with the output amplitude values dependent on the input amplitude value, an attribute of a typical nonlinear systems. The Euler angles are unstable.

A. *Linearized State-Space dynamics:*

The Jacobian linearization (16) is applied to system (13).

$$\dot{\underline{x}} = \frac{\partial \underline{F}(\underline{x},\underline{u})}{\partial \underline{x}}\underline{x} + \frac{\partial \underline{F}(\underline{x},\underline{u})}{\partial \underline{u}}\underline{u} \qquad (16)$$

Here $\frac{\partial \underline{F}}{\partial \underline{x}}$ is given by (17). Evaluating (17) at origin of state space and null input vector we get following linearized system dynamics (18).

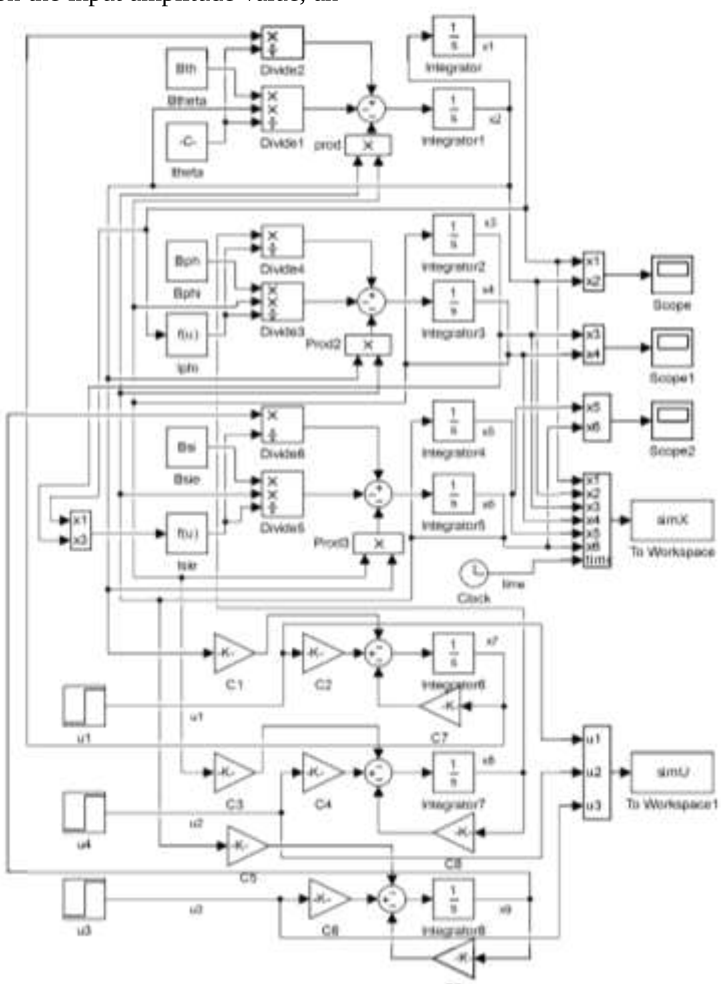

Figure 6. Nonlinear system simulation in SIMULINK.

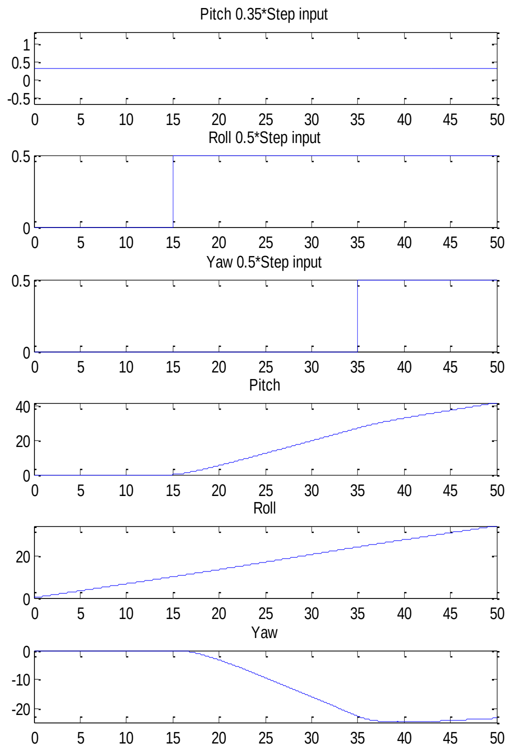

Figure 7. Step responses for the nonlinear system Euler angles.

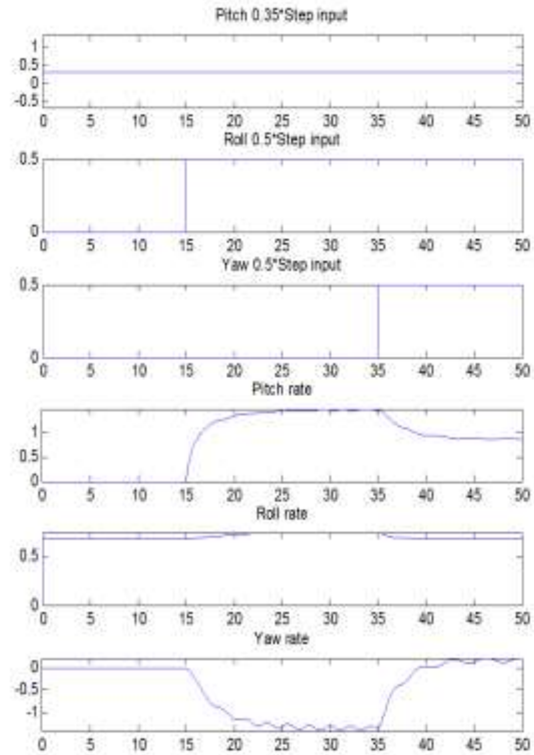

Figure 8. Step responses for the nonlinear system Euler rates.

$$\frac{\partial \underline{F}}{\partial \underline{x}} = \begin{bmatrix} 0 & 1 & 0 & 0 & 0 & 0 & 0 & 0 & 0 \\ 0 & -1.067 & 0 & -x_6 & 0 & -x_4 & 533.33 & 0 & 0 \\ 0 & 0 & 0 & 1 & 0 & 0 & 0 & 0 & 0 \\ f_1(\underline{x}) & -x_6 & 0 & f_2(\underline{x}) & 0 & -x_2 & 0 & f_3(\underline{x}) & 0 \\ 0 & 0 & 0 & 0 & 0 & 1 & 0 & 0 & 0 \\ 0 & -x_4 & f_5(\underline{x}) & -x_2 & 0 & f_6(\underline{x}) & 0 & 0 & f_7(\underline{x}) \\ 0 & -35.71 & 0 & 0 & 0 & 0 & -571.42 & 0 & 0 \\ f_4(\underline{x}) & 0 & 0 & -35.71 & 0 & 0 & 0 & -571.42 & 0 \\ 0 & 0 & 0 & 0 & 0 & -35.71 & 0 & 0 & -571.42 \end{bmatrix}$$

$$f_1(\underline{x}) = \frac{(x_4 - 250x_8)\cos x_1 \sin x_1}{23.43(\sin^2 x_1 + 18.44)^2},\ f_4(\underline{x}) = \frac{0.8181(x_9 - 0.006x_6)(\cos x_1 \sin x_1(1-\sin^2 x_3))}{\left[1+0.028(\sin^2 x_1 \sin^2 x_3 + \cos^2 x_1) + 0.46\sin^2 x_3 + 0.05\cos^2 x_3\right]^2}$$

$$f_2(\underline{x}) = \frac{-2.13}{\sin^2 x_1 + 18.4},\ f_5(\underline{x}) = \frac{0.8247(\cos x_3 \sin x_3(1+0.067\sin^2 x_1))(0.006x_6 - x_9)}{\left[1+0.028(\sin^2 x_1 \sin^2 x_3 + \cos^2 x_1) + 0.46\sin^2 x_3 + 0.05\cos^2 x_3\right]^2} \tag{17}$$

$$f_3(\underline{x}) = \frac{533.34}{\sin^2 x_1 + 18.4},\ f_6(\underline{x}) = \frac{-0.0886}{1+0.028(\sin^2 x_1 \sin^2 x_3 + \cos^2 x_1) + 0.46\sin^2 x_3 + 0.05\cos^2 x_3}$$

$$f_7(\underline{x}) = \frac{14.77}{1+0.028(\sin^2 x_1 \sin^2 x_3 + \cos^2 x_1) + 0.46\sin^2 x_3 + 0.05\cos^2 x_3}$$

$$A = \begin{bmatrix} 0 & 1 & 0 & 0 & 0 & 0 & 0 & 0 & 0 \\ 0 & -1.0667 & 0 & 0 & 0 & 0 & 533.34 & 0 & 0 \\ 0 & 0 & 0 & 1 & 0 & 0 & 0 & 0 & 0 \\ 0 & 0 & 0 & -0.1157 & 0 & 0 & 0 & 28.9157 & 0 \\ 0 & 0 & 0 & 0 & 0 & 1 & 0 & 0 & 0 \\ 0 & 0 & 0 & 0 & 0 & -0.0823 & 0 & 0 & 13.7159 \\ 0 & -35.7143 & 0 & 0 & 0 & 0 & -571.4286 & 0 & 0 \\ 0 & 0 & 0 & -35.7143 & 0 & 0 & 0 & -571.4286 & 0 \\ 0 & 0 & 0 & 0 & 0 & -35.7143 & 0 & 0 & -571.4286 \end{bmatrix}$$

$$B = \begin{bmatrix} 0 & 0 & 0 \\ 0 & 0 & 0 \\ 0 & 0 & 0 \\ 0 & 0 & 0 \\ 0 & 0 & 0 \\ 0 & 0 & 0 \\ 71.4286 & 0 & 0 \\ 0 & 71.4286 & 0 \\ 0 & 0 & 71.4286 \end{bmatrix}, C = \begin{bmatrix} 1 & 0 & 0 & 0 & 0 & 0 & 0 & 0 & 0 \\ 0 & 1 & 0 & 0 & 0 & 0 & 0 & 0 & 0 \\ 0 & 0 & 1 & 0 & 0 & 0 & 0 & 0 & 0 \\ 0 & 0 & 0 & 1 & 0 & 0 & 0 & 0 & 0 \\ 0 & 0 & 0 & 0 & 1 & 0 & 0 & 0 & 0 \\ 0 & 0 & 0 & 0 & 0 & 1 & 0 & 0 & 0 \end{bmatrix}, D = \begin{bmatrix} 0 & 0 & 0 \\ 0 & 0 & 0 \\ 0 & 0 & 0 \\ 0 & 0 & 0 \\ 0 & 0 & 0 \\ 0 & 0 & 0 \end{bmatrix} \quad (18)$$

1) Linear system simulation:

The step responses of the linear MIMO system (18) are shown in Fig. 9. The roll, pitch and yaw dynamics are unstable as expected. The Euler rate dynamics are stable, owing to the presence of back-EMF stabilization in PMDC motor dynamics. Moreover, the nondiagonal structure of the state matrix reveals the presence of coupling in the system dynamics (18).

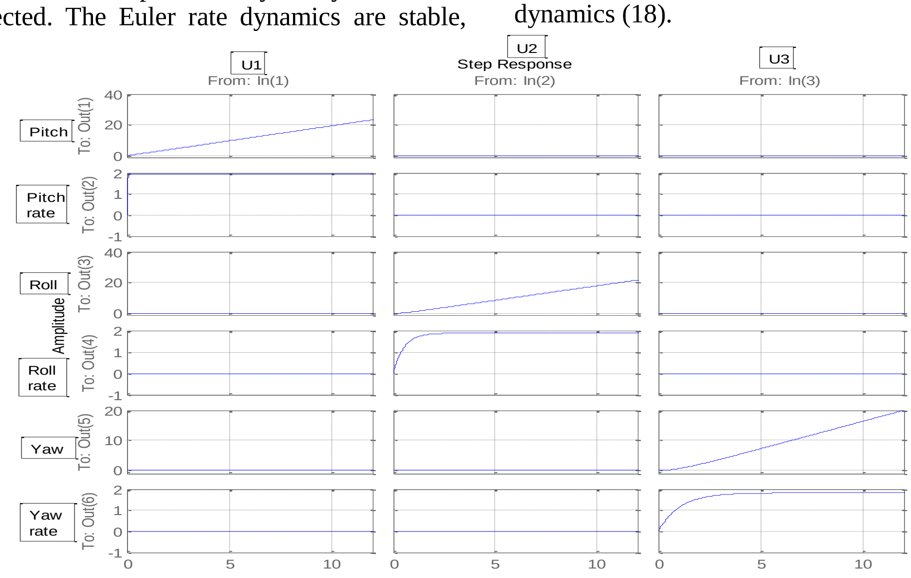

Figure 9. Linear system step responses.

IV. Discussions and Conclusions

In this part of the research work, we considered the detailed dynamics modeling of a 3-DoF gimbal stabilizing platform. The nonlinear system dynamics are simulated and linearized. The system dynamics are coupled and highly unstable. The further parts of this work will consider the Riccati-Sylvester differential transform to decouple the linear system dynamics derived here, followed by the control algorithm development to control the decoupled system.

References

[1] S. Paik, M. P. Nandakumar and S. Ashok, "Model development and adaptive control implementation of a 3-axis platform stabilization system," 2015 International Conference on Smart Technologies and Management for Computing, Communication, Controls, Energy and Materials (ICSTM), Chennai, 2015, pp. 526-531.

[2] G. Singh, M. P. Nandakumar and Ashok S, "Adaptive Fuzzy-PID and Neural network based object tracking using a 3-Axis platform," 2016 IEEE International Conference on Engineering and Technology (ICETECH), Coimbatore, 2016, pp. 1012-1017.

[3] M. R. Garzia, K. A. Loparo and C. F. Martin, "Disturbance decoupling, decentralized control and the Riccati equation," 1981 20th IEEE Conference on Decision and Control including the Symposium on Adaptive Processes, San Diego, CA, USA, 1981, pp. 1233-1235.

[4] J. Jin, "Observer design for satellite angular rate estimation using the state-dependent riccati equation method," in IEEE Transactions on Aerospace and Electronic Systems, vol. 51, no. 3, pp. 2496-2501, July 2015.

[5] T. Hamel and C. Samson, "Riccati observers for position and velocity bias estimation from direction measurements," 2016 IEEE 55th Conference on Decision and Control (CDC), Las Vegas, NV, USA, 2016, pp. 2047-2053.

[6] M. H. Korayem and S. R. Nekoo, "Suboptimal tracking control of nonlinear systems via state-dependent differential Riccati equation for robotic manipulators," 2015 3rd RSI International Conference on Robotics and Mechatronics (ICROM), Tehran, 2015, pp. 025-030.

[7] O. Biçer, M. U. Salamci and F. Kodalak, "State Dependent Riccati Equation based sliding mode control for nonlinear systems with mismatched uncertainities," 2016 17th International Carpathian Control Conference (ICCC), Tatranska Lomnica, 2016, pp. 54-59.

[8] X. Shen, Z. Gajic and M. T. Qureshi, "Reduced-Order Solution of the Weakly Coupled Matrix Difference Riccati Equation," 1991 American Control Conference, Boston, MA, USA, 1991, pp. 2437-2438

[9] D. K. Sharma, C. P. Sharma, S. S. Patel, B. A. Botre and S. A. Akbar, "Development of self-stabilizing 3-DOF -RRR camera system using fuzzy logic," 2015 Annual IEEE India Conference (INDICON), New Delhi, 2015, pp. 1-5.

[10] G. G. Redhyka, D. Setiawan and D. Soetraprawata, "Embedded sensor fusion and moving-average filter for Inertial Measurement Unit (IMU) on the microcontroller-based stabilized platform," 2015 International Conference on Automation, Cognitive Science, Optics, Micro Electro-Mechanical System, and Information Technology (ICACOMIT), Bandung, 2015, pp. 72-77.

[11] Z. Wei and S. Huiping, "Self-Adaptive Fuzzy Control of Multi-dim Vibration Using Parallel Mechanism with MR Dampers," 2009 International Conference on Information Technology and Computer Science, Kiev, 2009, pp. 464-467

[12] S. Leghmizi and S. Liu, "Takagi-Sugeno fuzzy PD controller for a 3-DOF stabilized platform," Proceedings of the 10th World Congress on Intelligent Control and Automation, Beijing, 2012, pp. 108-112